

On the Dynamics of Dip-Slip Fault Rupture Propagating at Supershear Speeds

Koji UENISHI^{1*}, Takayuki TAKAHASHI¹ and Koji FUJIMOTO¹

¹School of Engineering, The University of Tokyo (7-3-1 Hongo, Bunkyo, Tokyo 113-8656 Japan)

*E-mail: uenishi@dyn.t.u-tokyo.ac.jp

The mechanical details of dynamic dip-slip fault rupture causing earthquakes have not been fully clarified yet, because, first of all, the amount of available near-field seismological recordings is inadequate. Moreover, when the dip-slip fault plane is located near a free surface, the physical analysis near the propagating rupture tip becomes extremely complicated. Here, using the technique of finite difference modeling and laboratory dynamic photoelasticity, we show that the specific corner waves, i.e. energy-concentrated shear waves, may be generated in the hanging wall even when the initial upward fault rupture propagates at supershear speeds (larger than the relevant shear wave speed).

Key Words : *rock dynamics, dip-slip earthquake, supershear rupture, fracture dynamics, experimental mechanics*

1. INTRODUCTION

As mentioned in our earlier contributions¹⁾⁻²⁾, one noteworthy general feature associated with shallow dip-slip earthquakes is the nonsymmetric ground motions: The strong motion in the hanging wall is usually much larger than that in the footwall¹⁾⁻⁵⁾. However, the dynamic characteristics of dip-slip faulting near a free surface have not been completely understood yet and there is still no conclusive consensus regarding the reason for the abovementioned nonsymmetry. Here, in order to more comprehend the fracture dynamics of a dip-slip fault plane situated in a two-dimensional, monolithic linear elastic medium (e.g. rocks), we continue our numerical and experimental investigations using the PC-based finite difference technique and dynamic photoelasticity in conjunction with high speed cinematography. The evolution of dynamic wave field is recorded for the crack-like rupture along an interface (fault plane) in the model. The fracture experiments have been first motivated by the numerical prediction¹⁾ of the existence of the downward interface and corner waves related to dip-slip fault rupture at subsonic speeds, which shall be briefly summarized below.

2. SUPERSHEAR RUPTURE NEAR A FREE SURFACE: EXPERIMENTAL OBSERVATIONS

(1) Some background

In the numerical models employed during this series of finite difference simulations¹⁾⁻²⁾, a vertical or inclined fault plane has been set in a semi-infinite medium. In the vertical case (**Fig. 1(a)**), the initial remote static shear loading is assumed to increase in proportion to depth, and in the inclined case (dip angle 45 degrees; **Fig. 1(b)**), due to the action of the compressive normal stress, the static shear stress acting on the fault plane increases, again, linearly with depth. The seismic wave field (isochromatic fringe patterns) induced by fault rupture is obtained in the framework of linear elasticity, and without loss of generality, the longitudinal (P) wave speed V_P in the medium may be set as 1. If Poisson's ratio of the elastic medium is 0.25, the shear (S) and Rayleigh (R) wave speeds V_S and V_R are approximately 0.58 and 0.53, respectively. The orthogonal 201×201 grid points are used for the calculations, with the constant grid spacing 0.05 and time step 0.025. The crack-like rupture is initiated at time zero and it is propagated along the fault plane,

at a usual constant subsonic (and sub-Rayleigh) speed $V = 0.4 V_P$ ($\sim 0.69 V_S$) ($V < V_R < V_S < V_P$) for a total length 2 until it surfaces in the first series of numerical simulations. The corresponding Mach numbers related to this subsonic rupture are $M_P \equiv V/V_P = 0.4$ (< 1) and $M_S \equiv V/V_S \sim 0.69$ (< 1).

The isochromatic fringe patterns shown in **Fig. 1(c)** clearly indicate the strong rupture front waves near the upward moving tip and the static stress singularities at the other lower stationary tip of the rupturing fault plane at earlier stages. Upon total breakage of the fault plane, four Rayleigh surface wave-type waves are found to be generated: Two Rayleigh waves propagate along the free surface to the far-field (shown as R or R_h , R_f in the figure), and the other two interface waves (I) move downward back into depth along the already ruptured fault plane. The downward fault rupture after initial upward one seems to have existed⁶⁾ during the dynamic process of the 2011 off the Pacific coast of Tohoku, Japan, earthquake. Another important mechanical feature found here is the generation of the corner waves: When the fault plane is inclined (**Fig. 1(c)** right), the downward interface wave interacts with the Rayleigh surface wave (R_h) to cause a specific energy-concentrated shear wave, corner wave (C), and thus strong particle motions in the hanging wall. On the contrary, the weaker Rayleigh wave (R_f) controls the free surface particle motions and the interaction of this surface wave with the interface wave (I) is negligibly small in the footwall. The P and S waves in the footwall (P_f and S_f) are also much weaker than the corner wave in the hanging wall. In this way, the nonsymmetric particle motions associated with shallow dip-slip earthquakes may be induced.

In seismology, the existence of the downward interface wave (I) and the corner wave (C) has not been well appreciated yet, probably because these waves are not expected in ordinary earthquake source models with fault planes fracturing only at depth.

(2) Experimental observations

For the confirmation of the existence of downward interface waves and corner waves predicted by the numerical simulations in the previous section, dynamic photoelastic fracture experiments have

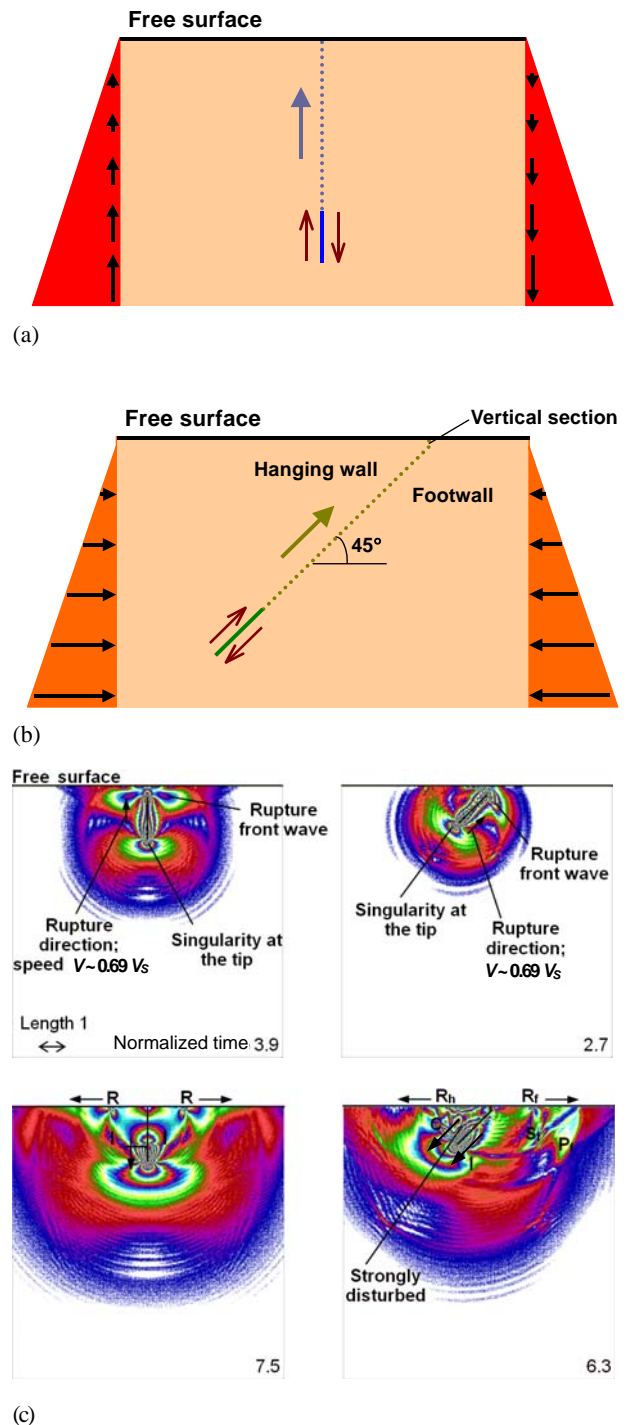


Fig. 1 The models employed for the numerical simulations of dip-slip fault rupture. (a) Vertical and (b) inclined cases. (c) Typical dynamic wave fields (isochromatic fringe patterns) generated numerically. The fringe order is proportional to the (normalized) maximum in-plane shear stress.

been performed in our laboratory²⁾. In each birefringent linear elastic polycarbonate specimen employed (Makrolon, 880 mm \times 200 mm \times 10 mm), an interface modeling a fault plane is pre-cut (but

welded). The experiments have been conducted without applying static stresses, and dynamic fracture is initiated upon impingement of a spherical projectile (diameter 6 mm, mass 0.2 grams) at a speed of 83 m/s and is propagated along the interface (**Figs. 2(a)** and **(b)**). The time-dependent evolution of dynamic wave field is recorded using a high speed digital video camera system (Photron FASTCAM SA5), this time at a frame rate of 75,000 frames per second. The P, S and Rayleigh wave speeds, V_P , V_S and V_R , in the polycarbonate plate are some 1,840, 810 and 760 m/s, respectively.

Figure 2(c) shows the isochromatic fringe patterns obtained experimentally. According to the photographs taken, the rupture speed V is in a “supershear” (transonic) range, and it is larger than V_S but smaller than V_P ($V_S < V < V_P$). The rupture speeds measured are $V \sim 1,600$ m/s for the vertical interface (**Fig. 2(c)** left) and 1,400 m/s for the inclined one (**Fig. 2(c)** right). That is, the Mach numbers of the rupture are $M_P \sim 0.76-0.87 (< 1)$ and $M_S \sim 1.73-1.98 (> 1)$, and more visually, the rupture front waves form Mach cones, which are sometimes called “shock waves” or Mach waves (see the pictures taken at relative time 0 μ s). Except that now the strong upward interface waves (I) moving along the fractured interface, not the rupture front waves themselves, may control the dynamic particle movements, the fundamental mechanical properties described in the previous section can be recognized also in the experimentally obtained photographs. The Rayleigh (R) and downward interface (I) waves can be found in the snapshot taken at time 160.00 μ s in the vertical interface case (**Fig. 3(c)** left)). Also, the numerically predicted corner wave (C) in the hanging wall is noticeable in the inclined interface case (at 226.67 μ s in **Fig. 3(c)** right).

3. NUMERICAL INVESTIGATION OF SUPERSHEAR DIP-SLIP FAULT RUPTURE

The experimentally recorded snapshots (**Fig. 2**) clearly show the corner and downward interface waves associated with supershear dip-slip faulting. Supershear rupture propagation is rather uncommon in conventional fracture mechanics, and in the

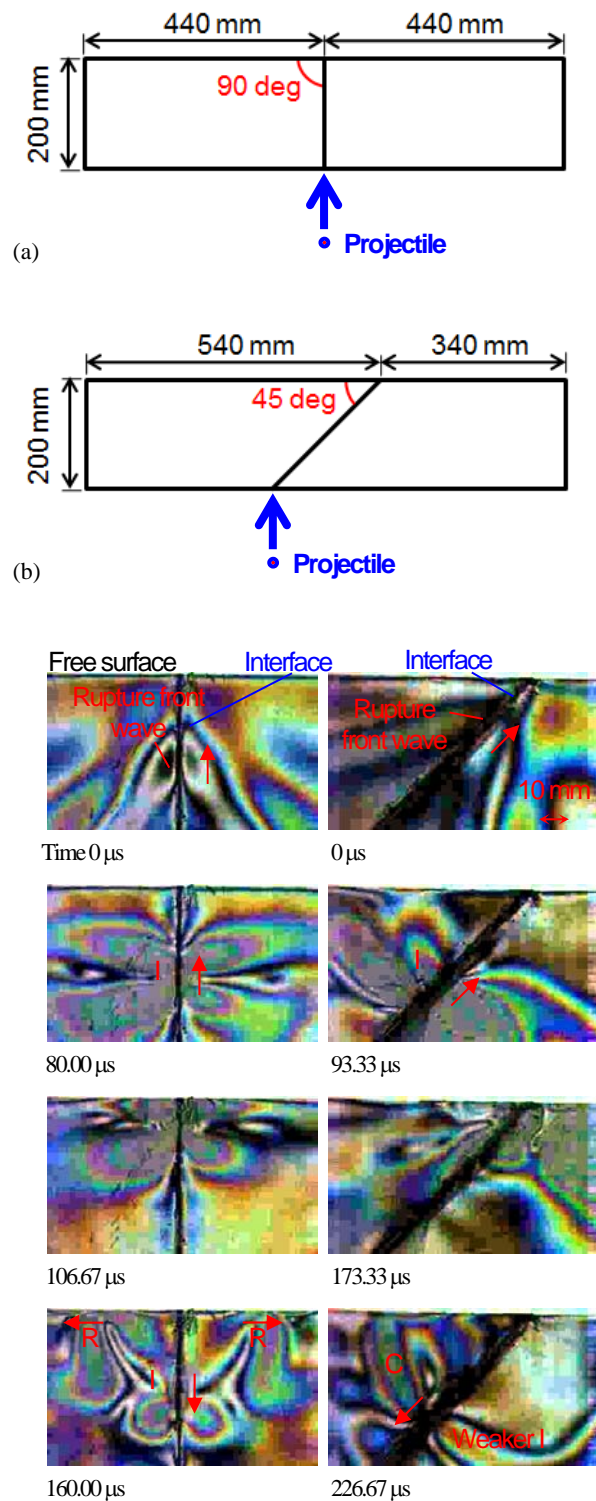
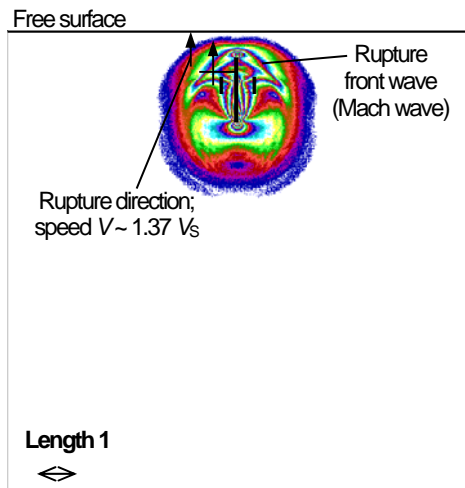
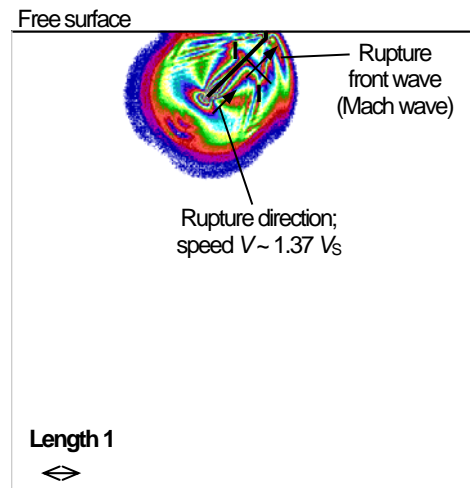


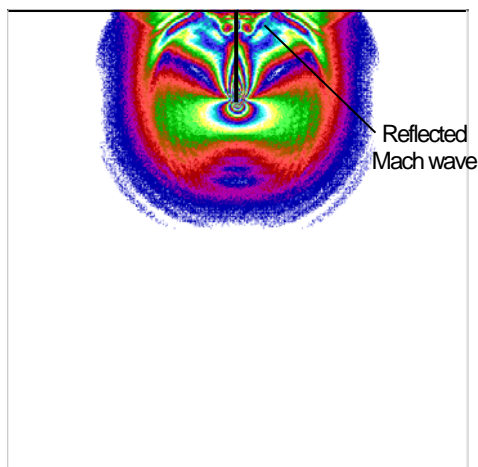
Fig. 2 Specimens used for the laboratory dynamic fracture experiments. In both (a) vertical and (b) inclined cases, the interfaces are initially welded. (c) Experimentally obtained isochromatic fringe patterns depicting supershear (transonic) rupture of an interface situated in the proximity of a free surface.



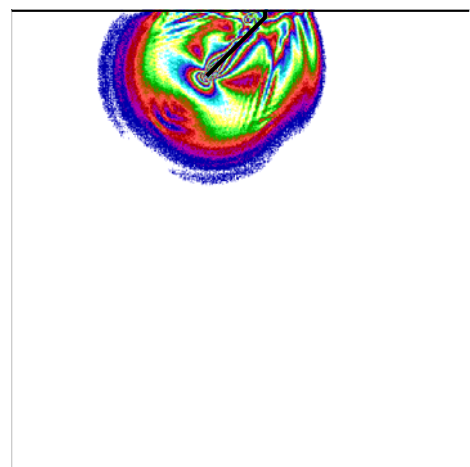
Normalized time 1.825



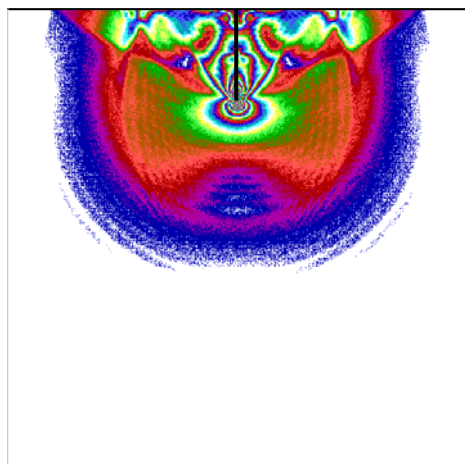
Normalized time 1.825



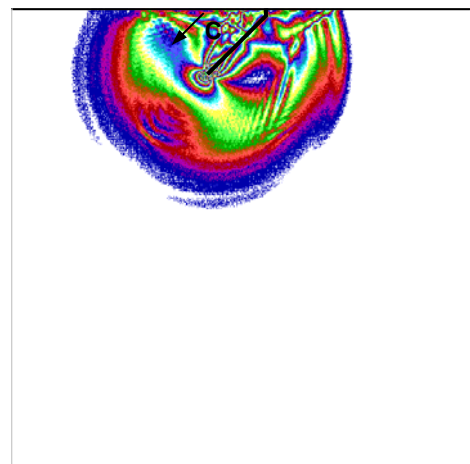
3.300



2.425



4.500



3.000

Fig. 3 Typical snapshots of the time-dependent isochromatic fringe patterns associated with the vertical supershear fault rupture that is initiated at depth and initially approaching the free surface.

Fig. 4 Numerically generated snapshots of isochromatic fringe patterns showing the initially upward supershear rupture along an inclined fault plane.

finite difference numerical calculations mentioned in ¹⁻²⁾, subsonic rupture speed is prescribed since this speed range is normally inferred from seismograms. However, supershear fault rupture is not rare in seismology⁷⁾, and in ²⁾, a preliminary result of the numerical study on supershear rupture has been briefly mentioned for a vertical fault plane. In this contribution, we further numerically investigate the supershear fault rupture using the same geometrical and material settings as shown in **Fig. 1** and including the case of the inclined fault plane. As before, in the simulations, the two-dimensional particle displacements at every orthogonal grid point are calculated at all time steps with the second order finite difference accuracy, and the energy absorbing conditions are satisfied at the outer three global (left, right and bottom) boundaries. At the top free surface, the vertical normal and tangential shear stresses are always assumed to be zero. Again, in all calculations, crack-like rupture propagation is presumed, but now, the rupture, initiated at time zero, moves along the fault plane with a prescribed constant supershear speed $V = (V_P + V_S)/2 \sim 0.79$ ($M_P \sim 0.79$, $M_S \sim 1.37$) until it surfaces.

For the case of dynamic rupture along a vertical fault plane shown in **Fig. 3**, not only the Mach-type rupture front wave but also the interface waves (I) moving more slowly upward along the fractured fault plane can be observed at normalized time 1.825, like in the experimentally obtained photographs. The Mach and interface waves may reach the free surface and reflected, and the Rayleigh and downward interface waves may be generated at later stages. The numerically obtained isochromatic fringe patterns compare well with those recorded during the experiments, but as mentioned above, the Rayleigh-type interface waves (I) propagating upward along the ruptured plane can be seen only under the supershear (and probably super-Rayleigh) rupture assumption (Compare **Fig. 1(c)** with **Figs. 2** and **3**).

Similarly, also in the case the fault plane is inclined (**Fig. 4**; dip angle 45 degrees), the rupture front wave forms a Mach cone, followed by the interface waves (I) at an earlier stage. These waves are reflected at the free surface and in the hanging wall, a corner wave (C) is generated and the

dynamic disturbance at normalized time 3.000 becomes much larger than that in the footwall. Thus, the experimental observations can be well reproduced in this new series of numerical simulations, and the nonsymmetric stress distributions and particle motions associated with the rupture of an inclined fault plane may be expected for both subsonic (sub-Rayleigh) and supershear (or super-Rayleigh) rupture speeds.

4. CONCLUSIONS

We have continued our numerical and experimental study on the wave field produced by dynamic rupture of a shallow dip-slip fault plane, and shown that surfacing fault rupture may generate Rayleigh surface waves moving along the free surface into the far field and another Rayleigh-type interface wave propagating back downward along the fractured fault plane. The study has also indicated that in the case of an inclined fault plane, the Rayleigh surface wave interferes with the downward interface wave to generate a strong shear corner wave and larger dynamic stresses in the hanging wall. The numerical and experimental models prepared in the study are simplified ones, and additional cautious numerical investigation can show that nonsymmetric particle motions can be induced even for the dynamic rupture of a geometrically symmetric vertical dip-slip fault plane when a layered structure⁸⁾ is introduced in the models. However, the existence of the downward interface waves as well as the corner waves looks confirmed by this series of laboratory fracture experiments, at least for the case of supershear upward rupture propagation. Currently, we are trying to conduct dynamic fracture experiments that may allow us to take the photographs of the corner waves generated by shallow dip-slip fault rupture propagation in a subsonic (sub-Rayleigh) range.

ACKNOWLEDGMENT: This study has been financially supported by the Ministry of Education, Culture, Sports, Science and Technology of Japan (MEXT) through the “KAKENHI: Grant-in-Aid for Scientific Research (C)” Program (No. 25420497).

KU is grateful to the continuous support provided by the Construction Engineering Research Institute Foundation in Kobe, Japan

REFERENCES

- 1) Uenishi, K., and Madariaga, R. I.: Surface breaking dip-slip fault: Its dynamics and generation of corner waves. *Eos Trans. AGU* 86, Fall Meet. Suppl., Abstract S34A-03, 2005.
- 2) Uenishi, K., Takahashi, T., and Fujimoto, K.: Fracture dynamics of shallow dip-slip earthquakes. *Proc. 2014 ISRM International Symposium and 8th Asian Rock Mech. Symposium*, in press, 2014.
- 3) Oglesby, D. D., Archuleta, R. J., and Nielsen, S. B.: Earthquakes on dipping faults; the effects of broken symmetry. *Science* 280, pp. 1055-1059, 1998.
- 4) Kao, H., and Chen, W.-P.: The Chi-Chi earthquake sequence: Active, out-of-sequence thrust faulting in Taiwan. *Science* 288, pp. 2346-2349, 2000.
- 5) Aoi, S., Kunugi, T., and Fujiwara, H.: Trampoline effect in extreme ground motion. *Science* 322, pp. 727-730, 2008.
- 6) Ide, S., Baltay, A., and Beroza, G. C.: Shallow dynamic overshoot and energetic deep rupture in the 2011 Mw 9.0 Tohoku-oki earthquake. *Science* 332, pp. 1426-1429, 2011.
- 7) Uenishi, K.: Supershear rupture propagation in a monolithic medium. *Proc. Twelfth Intl. Conf. on Fracture*, T15.006, 10 pages, 2009.
- 8) Uenishi, K.: Dynamic fracture in a layered medium induced by primary dip-slip fault rupture: Broken (anti-)symmetry. *Proc. 2014 Seismological Society of Japan Fall Meeting*, in press, 2014.